Arabian Journal of Chemistry (2023) **16**, 104955

King Saud University

Arabian Journal of Chemistry

www.ksu.edu.sa
www.sciencedirect.com

ORIGINAL ARTICLE

Chemical constituents and hepatoprotective properties of *Rhododendron simsii* Planch extract in Con A-induced autoimmune hepatitis

Fuqian Wang [a,b], Weiguang Sun [c], Zhou Lan [a], Yuan Zhou [a], Lulu Li [a,b], Ziheng Li [a], Ling Cheng [c,*], Qiuyun You [a,*], Qunfeng Yao [a,*]

[a] *Faculty of Pharmacy, Hubei University of Chinese Medicine, Wuhan 430065, Hubei, China*
[b] *Department of Pharmacy, Wuhan No.1 Hospital, Wuhan 430022, Hubei, China*
[c] *Hubei Key Laboratory of Natural Medicinal Chemistry and Resource Evaluation, School of Pharmacy, Tongji Medical College, Huazhong University of Science and Technology, Wuhan 430030, China*

Received 16 January 2023; accepted 25 April 2023
Available online 2 May 2023

KEYWORDS

Rhododendron simsii Planch;
AIH;
Flavonoid glycosides;
Network pharmacological;
NMR spectrum

Abstract *Rhododendron simsii* Planch, a folk medicine recorded in the 'Dictionary of Chinese Materia Medica', has been used by many ethnic regions of China to treat various inflammatory and immune-related diseases such as skin disorders and rheumatoid arthritis. However, its protective effect against autoimmune hepatitis and the underlying mechanisms remain unclear. The present study aimed to aimed to investigate the protective effects on autoimmune hepatitis through an integrated approach established by combining chemical composition identification, network pharmacology and *in vivo* experimental validation. Animal experiments showed that *R. simsii* Planch extract ameliorated ConA-induced liver injury, as evidenced by a reduction in ALT and AST levels and varying degrees of improvement in liver histopathology, with the *R-EE* (*R. simsii* Planch EtOAc extract) treated group showing the most obvious therapeutic effect. Then, chemical investigations into *R-EE* yielded 15 flavonoid and phenolic acid derivatives namely quercetin 3-O-α-L-rhamnoside (1), tamarixetin 3-rhamnoside (2), isoquercitrin (3), hyperoside (4), myricetin-3-O-α-L-rhamnopyranoside (5), afzelin (6), quercetin-3-O-α-L-arabinofuranoside (7), quercetin-3-O-α-D-arabinopyranoside (8), (+)-catechin (9), kaempferol (10), dihydromyricetin (11), quercetin

* Corresponding authors at: Hubei University of Chinese Medicine, No. 16 Huangjiahu West Road, Hongshan District, Wuhan, 430065, Hubei, China(Q. You, Q. Yao), Tongji Medical College, Huazhong University of Science and Technology, Hangkong Road 13, Wuhan, Hubei, China(L. Cheng).
E-mail addresses: wangfuqian.c@163.com (F. Wang), weiguang_sun@hust.edu.cn (W. Sun), lzlz_84@163.com (Z. Lan), zhouyuan03777@taihehospital.com (Y. Zhou), lilulu.zzu@163.com (L. Li), 554311656@qq.com (Z. Li), chengling630614@hust.edu.cn (L. Cheng), youqiuyun740723@hbtcm.edu.cn (Q. You), yaoqunfeng@hbtcm.edu.cn (Q. Yao).
Peer review under responsibility of King Saud University.

Production and hosting by Elsevier

https://doi.org/10.1016/j.arabjc.2023.104955

(12), vanillic acid (13), gallic acid (14) and farrerol (15). Further network pharmacological analysis indicated that the potential mechanism against ConA-induced liver injury is probably related to the regulation of the NF-κB signaling pathway. Experiments confirmed that R-*EE* could reduce liver damage and downregulate $CD4^+$ and inflammatory cytokine levels and the expressions of NLPR3, COX-2 and p-IκBα, and exhibited considerable hepatoprotective effects in ConA-induced AIH mice, which may be related to its flavonoids, and the underlying mechanism may involve the regulation of the NF-κB signaling pathway. The present results indicated that *R. simsii* Planch extract has more therapeutic potential in the treatment of autoimmune hepatitis, and provide the experimental basis for traditional application of *R simsii* Planch in the treatment of inflammatory diseases, and is a potential treatment agent for AIH that deserves further study.

1. Introduction

Autoimmune hepatitis (AIH) is an immunoinflammatory liver disease (Komori et al., 2021). An individual's susceptibility and development of AIH might be initiated by an extrinsic or intrinsic triggers, such as genetic factors (Herkel et al., 2020), viral infections (Mieli-Vergani et al., 2018) and drugs (Sebode et al., 2017). AIH associated chronic hepatocellular inflammation is characterized by parenchymal injury of liver tissue and extensive infiltration of inflammatory cells. This inflammatory disorder is accompanied by an elevation in serum transaminases, and inflammatory cytokines as well as dire hepatic necrosis and apoptosis which might result in hepatic cirrhosis, liver cancer and liver failure if no treatment is provided (Krawitt et al., 2006). Although, the pathogenesis and reasons for the development of AIH are not clear, the common idea is that potential intrinsic triggers relate to disorders of immune cells and costimulate inflammatory signals. $CD4^+$ T-cell responses with the production of interferon-γ (IFN-γ) and tumor necrosis factor-alpha (TNF-α) (Bovensiepen et al., 2019), and dysfunctional Tregs (Ferri et al., 2010) have been recognized as the key drivers of autoimmune pathology. Although significant progress has been made in understanding AIH pathogenesis, the lack of effective treatments remains a serious issue.

Concanavalin A (ConA) induced acute hepatitis in mice is a well-established model to induce AIH that simulates pathological alterations that occur in humans (Heymann et al., 2015; Ye et al., 2018). A single injection of ConA prompts infiltration of $CD4^+$ T helper cells into hepatic tissue concomitant with the generation of inflammatory cytokines such as TNF-α and interleukin-6 (IL-6) which in turn increase the level of reactive oxygen species (ROS) resulting in liver injury (Zhang et al., 2020).

In addition to $CD4^+$ T cells, Kupffer cells, natural killer T cells, and neutrophils account for inflammation in ConA-induced hepatitis (Wu et al., 2021). Recently, it has been clarified that nuclear factor kappa-B (NF-κB) is implicated in the progression of ConA-induced AIH. Upon instigation of NF-κB, upregulation of downstream inflammatory cascades takes place and accounts for the inflammation accompanying ConA (Jiang et al., 2022). The NLRP3 inflammasome is a cytoplasmic multiprotein complex involved in the occurrence and development of multiple diseases (Carta et al., 2015). Mounting evidence has shown that the NLRP3 inflammasome is expressed not only in innate immune cells (monocytes, macrophages, neutrophils, and dendritic cells) but also in nonimmune cells (hepatocytes, hepatic stellate cells, and endothelial cells) (Wree et al., 2014; et al., 2022). NLRP3 is a protein complex that is assembled by ASC and Caspase-1, thereby promoting the maturation of inflammatory factors (such as pro-IL-1β). NLRP3 inflammasome activation aggravates hepatic steatosis, hepatocyte inflammation, and fibrogenesis (Sun et al., 2019; Huang et al., 2021). Therefore, NLRP3 is a new therapeutic target for liver disease. Hence, NF-κB and NLPR3 signaling play important roles in the pathogenesis and therapy of AIH.

Traditional Chinese medicine (TCM) has achieved substantial curative effects in treating autoimmune disease (Ma et al., 2013; Wang et al., 2021). The *Rhododendron* genus, a member of the *Ericaceae* family, has rich resources and is distributed widely in China (Huang et al., 2018). Previously, many *Rhododendron* plants, such as *R. latoucheae* and *R. molle G*. Don have been reported to treat bronchitis, cough, rheumatoid arthritis, pain, and skin ailments (Popescu et al., 2013; Liu et al., 2018; Luo et al., 1993), and applied on chronic glomerular nephritis therapy as folk medicine (Liu et al., 2005). *R. molle* G. Don was recorded in 'Shennong's Classic of Materia Medica' and used as an anesthetic. *R. simsii* Planch, also known as Ying-shanhong, is a folk medicine recorded in the 'Dictionary of Chinese Materia Medica' and 'Compendium of Materia Medica' for treating rheumatic diseases. It has also been used by many ethnic communities in China to control cough, pain, and various inflammatory and immune-related diseases such as rheumatoid arthritis. (Nanjing University of Traditional Chinese Medicine, 2006). Previous studies suggested that total flavones of *Rhododendron simsii* Planch (total flavones of *Rhododendra* TFR) have neuroprotective and protective effects on ischaemia–reperfusion injury (Guo et al., 2020; Sun et al., 2018). TFR has a significant protective effect on ischemia and reperfusion injury in rat heart, which is related to inhibiting the expression of NF-κB, TNF-α and ICAM-1, as well as reducing SOD and myeloperoxidase (MPO) activities (Zhang et al., 2007). The analgesic and anti-inflammatory effects of TFR may be related to inhibiting the production of PGE2 (Song et al., 2007; Song et al., 2006). TFR also has antitussive and asthmatic effects (Wang et al., 2006), and the efficiency of chronic bronchitis treatment with a preparation of *R. simsii* Planch was 91.9% in 1132 cases. (Chinese Herbal Medicine Research Group, Training Department, Second Military Medical University, 1978). AIH is an immunoinflammatory liver disease associated with chronic hepatocellular inflammation and extensive infiltration of inflammatory cells. Inspired by the traditional application of *R. simsii* Planch in the treatment of inflammatory and immune-related diseases such as rheumatoid arthritis, we investigated the protective effect of *R. simsii* Planch against autoimmune hepatitis induced by Con A.

In the present study, we investigated the protective effects of different extracts of *Rhododendron simsii* Planch on ConA induced acute live injury in mice. Based on the isolation and identification of chemical components, we further elucidated the potential molecular mechanism of *R-EE* against AIH with the help of network pharmacology and experimental validation.

2. Materials and methods

2.1. Chemicals, reagents, and animals

Con A was purchased from Sigma-Aldrich (St. Louis, USA). Alanine aminotransferase (ALT) and aspartate transaminase (AST) kits were purchased from Nanjing Jiancheng Biological

Product (Nanjing, China). The cytokine enzyme-linked immunosorbent assay (ELISA) kits were from Boster Biological Technology Co. Ltd (Wuhan, China). Antibodies against NLPR3, COX-2, IκBα and p-IκBα were purchased from Cell Signaling Technology, Inc. (Beverly, MA, USA).

Male C57BL/6J (B6) mice (20–24 g) were purchased from Beijing HFK Bioscience (China). All mice were housed under specific pathogen-free (SPF) conditions and allowed free access to water and food. In this study, all procedures involving animals were performed and monitored in compliance with the guidelines of Tongji Animal Use Regulations and approved by the Institutional Animal Care and Use Committee of Tongji Medical College (IACUC Number: 2881).

2.2. Plant materials, extraction and fractionation

The leaves of *Rhododendron simsii* Planch were collected from Shennongjia in Hubei Province, China, and identified by Prof. Xincai Hao (*Hubei University of Medicine, Shiyan, China*). A voucher specimen (No. Pharm-202006) was deposited at the Department of Pharmacy, Wuhan First Hospital for future reference. The air-dried leaves (20 kg) were extracted with 95% aqueous EtOH (each 2-day, 50 L × 3 times) at room temperature. The filtrates were combined and concentrated under vacuum to afford the crude extract, which was suspended in H_2O (6 L) and then successively re-extracted with chloroform, EtOAc and n-BuOH (5 L × 4). Each solvent was concentrated under vacuum separately to afford 516 g (dichloromethane, *R-DE*), 230 g (EtOAc, *R-EE*), 575 g (n-BuOH, *R-BE*), and 910 g (H_2O, *R-WE*) residue. The obtained extract was stored in a refrigerator at 4 °C until use.

2.3. Model preparation

Concanavalin A (ConA) induced autoimmune hepatitis is a classical and acute T-cell-mediated hepatic immunological injury. Administration of ConA induced pathological damage and inflammatory infiltration of the liver in 8–16 h. Thus, the conA-induced autoimmune hepatitis model was chosen according to a previous report with some modifications (Heymann et al., 2015; Ye et al., 2018; Zhang et al., 2020; Wu et al., 2021). Mice were randomly divided into ten groups (n = 6 each group): control group, ConA model group and the four different extractions (*R-DE*, *R-EE*, *R-BE*, and *R-WE*,) with 25 and 50 mg/kg groups. ConA was dissolved in pyrogen-free phosphate-buffered saline (PBS) and intravenously injected at 15 mg/kg to induce liver injury. The extracts (dissolved in saline solution) were intragastrically administered to animals for 5 days before the ConA injection. All mice were sacrificed at 12 h after Con A injection using anesthesia with 1% pentobarbital (10 mL/kg). Serum and liver tissues were harvested and stored at −80 °C.

2.4. Measurement of serum levels of ALT and AST

Blood samples were harvested by drawing blood from the eyeball. Serum samples were then isolated from the blood by centrifugation at 3000 rpm for 15 min, after blood coagulation for 2 h on ice. The activities of ALT and AST in serum were measured using commercial kits from Nanjing Jiancheng Bioengineering Institute (Nanjing, China), according to the manufacturer's instructions.

2.5. Assessment of liver histopathology

The isolated left lateral liver lobes were fixed in 4 % formaldehyde. After the tissues were embedded in paraffin, the tissue sections were obtained and stained with hematoxylin and eosin (HE). The specimens were examined under light microscopy.

2.6. TUNEL assay

Terminal deoxynucleotidyl transferase-mediated dUTP nick end labeling (TUNEL) assays were performed with an In Situ Cell Death Detection Kit, TMR red (Roche, NJ, USA), according to the manufacturer's instructions. Liver samples were treated as described in the assessment of liver histopathology section. Briefly, the liver tissue sections were pretreated with 0.1% Triton X-100 for 8 min, washed with PBS buffer, and then stained with TUNEL reaction mix for 1 h at 37 °C.

2.7. HPLC analysis and isolation

2.7.1. HPLC analysis

The quality of the *R-EE* was measured on a DIONEX UItiMate 3000 HPLC system, using a C_{18} column (Waters Xbridge 4.6 × 150 mm, 5 μm); the mobile phase composition was methanol (A) and 0.04%(V/V) formic acid aqueous solution (B) (A: 10–90% in 35 min, 100% in 40–50 min); flow rate: 1 mL/min; temperature: 35 °C; detective wavelength: 250 nm.

2.7.2. Isolation

The *R-EE* (46 g), flavonoid-rich fraction, was chromatographed by MPLC with an EZ Plus 100D chromatography system (Sepaflash spherical C18, 40–75 μm, 100 Å, 300 psi) eluted with a MeOH/H_2O (methanol: 25%–100% in 75 min; 100% in 75–90 min; flow rate: 20 mL/min) gradient to give ninety samples 1–90 (concentrated by SpeedVac SPD2030, Thermo Fisher Scientific). Subsequently, the samples were chromatographed over Sephadex LH-20, and similar components were combined under thin-layer chromatography (TLC) analysis, to afford 27 subfractions (sub-Frs 1–27). According to the chromatographic analysis of chemical components (including most of the major chromatographic peaks), subfractions 4, 16, 21 and 27 were selected for further separation.

Sub-Fr 21 was separated by preparative chromatography (Waters 2535; Waters SunFire^{TM} C_{18} OBD^{TM}, 5 μm, 19 × 150 mm; methanol: 15–75% in 30 min; 100% in 30–35 min; flow rate: 10 mL min^{-1}) and subsequently further separated by semipreparative HPLC (DIONEX UItiMate 3000 HPLC system, YMC-Pack ODS-AQ, 5 μm, 10 × 250 mm, 3 mL min^{-1}) to afford Compounds 14 (216.3 mg, t_R = 6.8 min, MeOH-H_2O, 25:75, 0.2% FA), 9 (208.4 mg, t_R = 12.5 min, MeOH-H_2O, 25:75, 0.2%FA), 12 (6.7 mg, t_R = 11.5 min, MeOH-H_2O, 60:40, 0.2% FA), 8 (99.0 mg, t_R = 29.0 min, MeOH-H_2O, 42:58, 0.2% FA), 7 (122.6 mg, t_R = 32.3 min, MeOH-H_2O, 43:57, 0.2%FA), 6 (191.0 mg, t_R = 42.2 min, ACN-H_2O, 20:80, 0.2% FA), 5 (192.9 mg, t_R = 14.99 min, ACN-H_2O, 20:80, 0.2% FA), 4 (41.7 mg, t_R = 15.5 min,

ACN-H_2O, 20:80, 0.2% FA), 3 (5.2 mg, t_R = 16.6 min, ACN-H_2O, 20:80, 0.2% FA), 1 (1712.2 mg, t_R = 23.2 min, ACN-H_2O, 20:80, 0.2% FA), and 2 (115.3 mg, t_R = 51.0 min, ACN-H_2O, 20:80, 0.2% FA). Similarly, Compounds 11 (347.1 mg, t_R = 19.8 min, ACN-H_2O, 16:84, 0.2% FA) and 10 (8.2 mg, t_R = 12.8 min, MeOH-H_2O, 35:75, 0.2% FA) were obtained from sub-Fr 16, and Compound 13 (106.6 mg, t_R = 23.0 min, MeOH-H_2O, 25:75, 0.2% FA) was obtained from sub-Fr 4. Sub-Fr 27 was further purified by column chromatography over Sephadex LH-20 eluting with MeOH to yield Compound 15 (86.2 mg). NMR spectra were recorded on 400 M or 600 M Bruker spectrometers in DMSO d_6 or CD_3OD.

2.8. Ingredient-target interaction network construction and analysis

The potential targets of *R-EE* for treating AIH were obtained from the traditional Chinese medicine systems pharmacology database (TCMSP) (Ru et al., 2014) based on the identified ingredients from *R-EE*, and overlapped with AIH-related gene targets from the GeneCards database (Safran et al., 2003). The following visual processing was performed by employing Cytoscape 3.8.2 analysis of ingredient-target interaction network to screen core targets based on degree centrality (DC).

2.9. Enrichment of GO terms and KEGG pathways

To explore the potential signaling pathways, biological processes (BP), molecular function (MF), or cell component (CC) regulated by *R-EE*, we performed gene ontology (GO) function enrichment analysis using Database for Annotation, Visualization and Integrated Discovery (https://david.ncifcrf.GOv/tools.jsp, Ver. 6.8). The top 20 enriched terms were visualized using an online tool (https://www.bioinformatics.com.cn). We also used pathway data obtained from the KEGG database for pathway enrichment analysis. Focusing on the effect of AIH, the top 20 enriched signaling pathways were visualized.

2.10. Determination of serum cytokine levels by ELISA

IL-1β, IFN-γ and TNF-α levels were measured by enzyme-linked immunosorbent assay (ELISA), using commercial kits from Boster Biological Technology Co. Ltd (Wuhan, China). All procedures were carried out according to the protocols provided by the manufacturers.

2.11. Quantitative real-time PCR

Total RNA was extracted from liver tissues by TRIzol (Shanghai Yeasen Biotechnology Co., Ltd., Shanghai, China). RNA was reverse - transcribed into single-strand cDNA by using a reverse transcription system kit (Applied Biological Materials Inc, Vancouver, Canada). The mRNA levels were measured by quantitative real-time PCR (qRT-PCR) using SYBR Green qPCR Master Mix (Bimake, Houston, TX, USA) on a QuantStudio™ 3 System (Applied Biosystems, California, USA) according to the manufacturer's protocol. The primers are listed in Table 1.

Table 1 Primer used for qRT-PCR.

Gene		Squences
IFN	F	CTACTCATTCACCAGCAAGAT
	R	CCATTCCTTCTTGGGGTCA
TNF-α	F	CCCTCCTGGCCAACGGCATG
	R	TCGGGGCAGCCTTGTCCCTT
IL-1β	F	GGCAGGCAGTATCACTCATT
	R	GAAGGTGCTCATGTCCTCATC
β-actin	F	CGTGCGTGACATCAAAGAGAA
	R	TGGATGCCACAGGATTCCAT

2.12. Liver histological evaluation and immunohistochemistry analysis

The fixed liver tissues of the control, model and *R-EE* treatment groups were sent for further immunohistochemical staining of $CD4^+$ and NLPR3. The sections were scanned using the digital slide scanner NanoZoomer 2.0 RS (Hamamatsu, Massy, France). Corresponding positive cells were calculated with Image-Pro Plus 6.0 software.

2.13. Western blotting analysis

Protein concentrations were determined using a BCA protein assay kit (Beyotime Biotech, Shanghai, China). Nuclear proteins were used for to determine NLPR3, COX-2, IκBα and p-IκBα protein levels. The same amount of sample proteins, 30 μg per lane, was separated by 12% SDS-polyacrylamide gel electrophoresis (PAGE) and transferred to a PVDF membrane (Millipore, Bedford, USA). The membrane was blocked with 5% fat-free milk in TTBS buffer, and then incubated at 4 °C overnight, with a proper primary antibody. The membranes were further washed with TTBS buffer three times, and incubated with HRP-conjugated secondary antibodies at 37 °C for 2 h. After incubation with the secondary antibody, proteins were detected with an ECL chemiluminescence detection kit. The amount of protein expression was normalized to the amount of β-actin in the same sample.

2.14. Statistical analysis

All the data in this study are presented as the means ± SEMs. Statistical analysis was carried out by using GraphPad Prism 6. Student's *t* test was performed between two groups and one-way analysis of variance with Student–Newman–Kuels multiple comparison was used for experiments involving more than two groups. $p < 0.05$ was considered statistically significant.

3. Results

3.1. Effects of *Rhododendron simsii* Planch on ConA-induced liver injury

To evaluate the effect of *Rhododendron simsii* Planch in the ConA-induced liver injury, ConA-induced hepatitis model in mice was successfully established. Firstly after 5 days of extraction treatment, all the animals had no obvious toxic reaction

Table 2 ^{1}H NMR data of compounds 1–8 (400 MHz, *J* in Hz).

no	1	2	3	4	5	6	7	8
6	6.22 (d, 1.9)	6.40 (d, 1.8)	6.21 (d)	6.23 (d, 1.9)	6.22 (d, 2.1)	6.23 (d, 2.0)	6.20 (d, 2.1)	6.19 (d, 1.7)
8	6.39 (d, 1.9)	6.23 (d, 1.9)	6.41 (s)	6.43 (d, 1.7)	6.39 (d, 2.1)	6.41 (d, 1.9)	6.39 (d, 2.0)	6.39 (s)
1′								
2′	7.36 (d, 2.0)	7.36 (d, 2.1)	7.73 (d, 2.1)	7.87 (d, 2.0)	6.97 (s)	7.79 (d, 8.7)	7.52 (d, 2.1)	7.74 (d, 2.1)
3′						6.96 (d, 8.8)		
5′	6.93 (d, 8.3)	7.10 (d, 8.5)	6.89 (d, 8.5)	6.89 (d, 8.5)		6.96 (d, 8.8)	6.89 (d, 8.3)	6.86 (d, 8.5)
6′	7.33 (dd, 8.3, 2.0)	7.44 (dd, 8.5, 2.1)	7.61 (dd, 8.5, 2.0)	7.61 (dd, 8.5, 2.1)	6.97 (s)	7.79 (d, 8.7)	7.49 (dd, 8.3, 2.2)	7.57 (dd, 8.5, 2.0)
1″	5.37 (d, 1.4)	5.40 (d, 1.5)	5.29 (d, 7.5)	5.19 (d, 7.8)	5.33 (d, 1.4)	5.40 (d, 1.6)	5.46 (s)	5.15 (d, 6.6)
2″	3.77 (dd, 9.3, 3.3)	4.24 (dd, 3.2, 1.6)	3.51 (m)	3.83 (d, 8.0)	4.24 (dd, 3.2, 1.7)	4.24 (dd, 3.3, 1.7)	4.32 (dd, 3.0, 0.9)	3.89 (dd, 8.4, 6.7)
3″	3.46 (m)	3.75 (dd, 9.0, 3.3)	3.45 (t, 8.8)	3.58 (m)	3.81 (dd, 9.5, 3.3)	3.73 (d, 5.8)	3.90 (dd, 5.2, 3.0)	3.64 (dd, 8.4, 3.0)
4″	3.37 (m)	3.35 (m)	3.34 (t, 10.0)	3.88 (d, 3.2)	3.37 (m)	3.33 (m)	3.84 (q, 4.7)	3.80 (m, overlap)
5″*a*	4.24 (dd, 3.1, 1.4)	3.35 (m)	3.4 (m)	3.50 (t, 6.0)	3.54 (m)	3.35 (m)	3.49 (dd, 4.1, 2.0)	3.82 (m, overlap)
5″*b*								3.44 (m)
6″*a*	0.96 (d, 6.1)	0.95 (d, 5.5)	3.74 (dd, 11.9, 2.1)	3.67 (dd, 11.2, 6.0)	0.98 (d, 6.2)	0.94 (d, 5.6)		
6″*b*			3.60 (dd, 11.9, 5.3)	3.57 (m)				

record in CD_3OD.

Table 3 ^{1}H NMR data of compounds 9–15 (400 MHz, *J* in Hz).

No	9	10	11	12	13	14	15
2	4.58 (d, 7.5)		4.85 (d, 11.4)		7.57 (d, 8.7)	6.93 (s)	5.30 (d, 12.8)
3	3.99 (td, 7.9, 5.4)		4.48 (d, 11.4)		6.85 (d, 8.7)		3.06 (dd, 16.9, 12.9)
							2.71 (dd, 16.9, 2.2)
4*a*	2.87 (dd, 16.1, 5.4)						
4*b*	2.52 (dd, 16.1, 8.2)						
6	5.95 (d, 2.3)	6.20 (d, 1.7)	5.90 (d, 2.1)	6.19 (s)	7.58 (s)	6.93 (s)	
8	5.87 (d, 2.2)	6.42 (s)	5.94 (d, 2.1)	6.40 (s)			
2′	6.86 (d, 1.9)	8.11 (d, 8.6)	6.54 (s)	7.76 (s)			7.32 (d, 8.2)
3′		6.93 (d, 8.9)					6.82 (d, 8.6)
5′	6.78 (d, 8.1)	6.93 (d, 8.9)		6.91 (d, 8.5)			6.82 (d, 8.6)
6′	6.74 (dd, 8.1, 1.9)	8.11 (d, 8.6)	6.54 (s)	7.66 (d, 8.3)			7.32 (d, 8.2)
3,5-OH						9.22 (s)	
4-OH						8.87 (s)	
6-Me							2.00 (s)
8-Me							1.99 (s)
-OMe					3.91 (s)		
–COOH						12.27 (s)	

All except 14 (DMSO d_6) are record in CD_3OD.

with normal eating and playing as previous. Then we assessed the serum ALT and AST levels and histopathological changes in livers after 12 h of challenge with ConA. As shown in Fig. 1A, morphological abnormalities were observed in the Con A group, including extensive vacuolization with the loss of liver architecture, congestion, lymphocytic infiltration and large area necrosis, which displayed severe liver injury induced by Con A. In contrast, pretreatment with different extracts effectively prevented the microscopic disruptions and hepatocyte necrosis induced by Con A to varying degrees; specifically, the histology of the 50 mg/kg *R-EE* treated group was close to that of the normal liver, which showed the most significant therapeutic effect. Compared with *R-EE*, *R-DE* also showed a similar effect on ameliorating hepatocyte necrosis as well as serum AST and ALT levels, while *R-BE*, and *R-WE* showed a weaker effect.

TUNEL staining is a classical non-isotopic method to detect DNA fragmentation in cells during apoptosis, which can quickly and accurately detect single apoptotic cells. Hepatocyte apoptosis is another important manifestation in the Con A-induced liver injury model. Thus, TUNEL staining of the liver sections were carried out to clarify the effect of extracts

Table 4 ^{13}C NMR data of compounds 1–15 (600 MHz, *J* in Hz).

no	1	2	3	4	5	6	7	8	9	10	11	12	13	14	15
1													123.3	120.9	
2	158.5	158.9	158.6	158.8	159.9	159.4	159.5	159.0	83.0	148.2	85.4	148.1	125.4	109.2	80.1
3	136.2	136.4	135.7	136.0	136.4	136.4	135.0	136.2	68.9	137.4	73.8	137.3	115.9	145.8	44.1
4	179.6	179.6	179.6	179.8	179.8	179.8	180.1	180.0	28.7	177.6	198.4	177.4	152.8	138.4	198.4
5	159.3	158.6	163.2	163.3	163.4	163.4	163.2	163.6	157.9	162.6	165.5	162.6	148.8	145.8	160.3
6	99.8	94.7	100.0	100.3	99.9	99.9	100.0	100.5	96.4	99.4	97.4	99.5	113.9	109.2	104.8
7	165.9	166.0	166.2	159.1	166.1	166.1	166.2	166.7	157.7	165.7	168.8	166.2			159.7
8	94.7	99.9	94.8	95.0	94.8	94.9	94.9	95.3	95.6	94.6	96.4	94.6			103.3
9	163.2	163.2	159.1	159.1	158.6	158.7	158.7	159.2	157.0	158.4	164.6	158.4			164.1
10	105.9	105.9	105.8	105.9	105.9	106.1	105.7	106.1	100.9	104.7	101.9	104.5			104.1
1′	122.9	124.3	123.3	123.3	122.0	122.8	123.1	123.6	132.3	123.9	129.2	124.3			131.5
2′	116.3	116.6	116.1	116.4	109.7	132.0	116.9	118.0	115.4	130.8	108.1	116.1			128.8
3′	146.4	147.7	150.0	146.1	147.0	116.7	146.5	146.5	146.4	116.4	147.0	148.9			116.3
4′	149.8	151.6	146.0	150.2	138.0	161.7	150.0	150.5	146.5	160.1	135.0	146.3			158.9
5′	116.9	112.4	117.7	118.1	147.0	116.7	116.6	116.7	116.2	116.4	147.0	116.4			116.3
6′	122.8	122.7	123.2	123.2	109.7	132.0	123.2	123.4	120.2	130.8	108.1	121.8			128.8
1″	103.5	103.5	104.4	105.7	103.8	103.6	109.6	105.2							
2″	72.0	71.9	75.8	73.5	72.2	72.1	83.5	73.4							
3″	72.1	72.0	78.2	75.4	72.1	72.3	78.8	74.7							
4″	73.2	72.1	71.3	70.3	73.5	73.3	88.1	69.7							
5″	71.9	73.2	78.5	77.5	72.0	72.2	62.7	67.5							
6″	17.6	17.7	62.7	62.2	17.8	17.8									
4′-OMe		56.4													
5-OMe													56.5		
6-Me															8.1
8-Me															7.4
COOH													170.3	167.9	

All except 14 (DMSO d_6) are record in CD_3OD.

on ConA-induced hepatocyte apoptosis in mice. As shown in Fig. 1B, massive hepatocyte apoptosis was observed in the livers of mice in the Model group. *R-EE* pretreatment dramatically attenuated ConA-induced hepatocyte apoptosis in the liver compared with the model group, which suggests that *R-EE* prevented hepatocyte apoptosis in ConA-induced hepatitis.

Serum ALT and AST levels were used to estimate the degree of liver damage. We found that serum ALT and AST clearly increased 12 h after ConA administration compared with the control group ($P < 0.001$). Moreover, *R-EE* pretreatment significantly attenuated the serum levels of ALT and AST induced by ConA, which was consistent with the HE and TUNEL analyses ($P < 0.05$) (Fig. 1C, D). These results showed that *R-EE* has a protective role in ConA-induced liver injury.

3.2. HPLC analysis and structure elucidation

The crude extract was fractionated by successive re-extraction with different solvents affording five fractions. After hepatoprotective activity evaluation, HPLC analysis of the EtOAc fraction (*R-EE*) was performed and 15 major chromatographic peaks were observed (Fig. 2). Then, *R-EE* was chromatographed, and subfractions of interest were further purified to yield Compounds 1–15. The compounds were isolated as yellow or colorless powders with dark spots under UV light at 254 nm and dark green spots after spraying with $FeCl_3$ reagent, which indicated that the compounds were phenolic compounds. Their structures were identified based on spectroscopic data analysis and comparison with their spectral data reported in the literature Fig. 3. ^1H and ^{13}C data are delineated in the supplementary material (S31-33)Table 2-4. Grayanane diterpenes were reported to be toxic components of plants in *Ericaceae* (Wang et al., 2014; Li et al., 2013). However, the results of phytochemical investigation indicated that the main components of *R-EE* in this study are flavonoids.

3.3. Network pharmacology analysis

A total of 175 potential pathophysiological targets of the compounds were obtained from the TCMSP database, including PTGS2, PTGS1, NCOA2, PPARG and NOS3, 148 of which intersected with AIH-related targets from the GeneCards database (Supplementary Table 1). To comprehensively identify the mechanism by which *R-EE* treats AIH, we constructed a network between ingredients isolated from the extract and their correspondent targets (Fig. 4). In the network, targets in the inner circle are more closely linked with ingredients than those in the outer circle. PTGS (prostaglandin-endoperoxide synthase) 2, a key enzymethat regulates immunity, inflammation, and cell proliferation, was influenced by 11 ingredients through the TNF and IL-17 signaling pathways. At the same time, PPARG and NOS3 were tuned by 4 ingredients.

3.4. Biological enrichment and pathway analysis

The potential targets were assayed for functional prediction via GO enrichment analysis. The GO analysis results showed

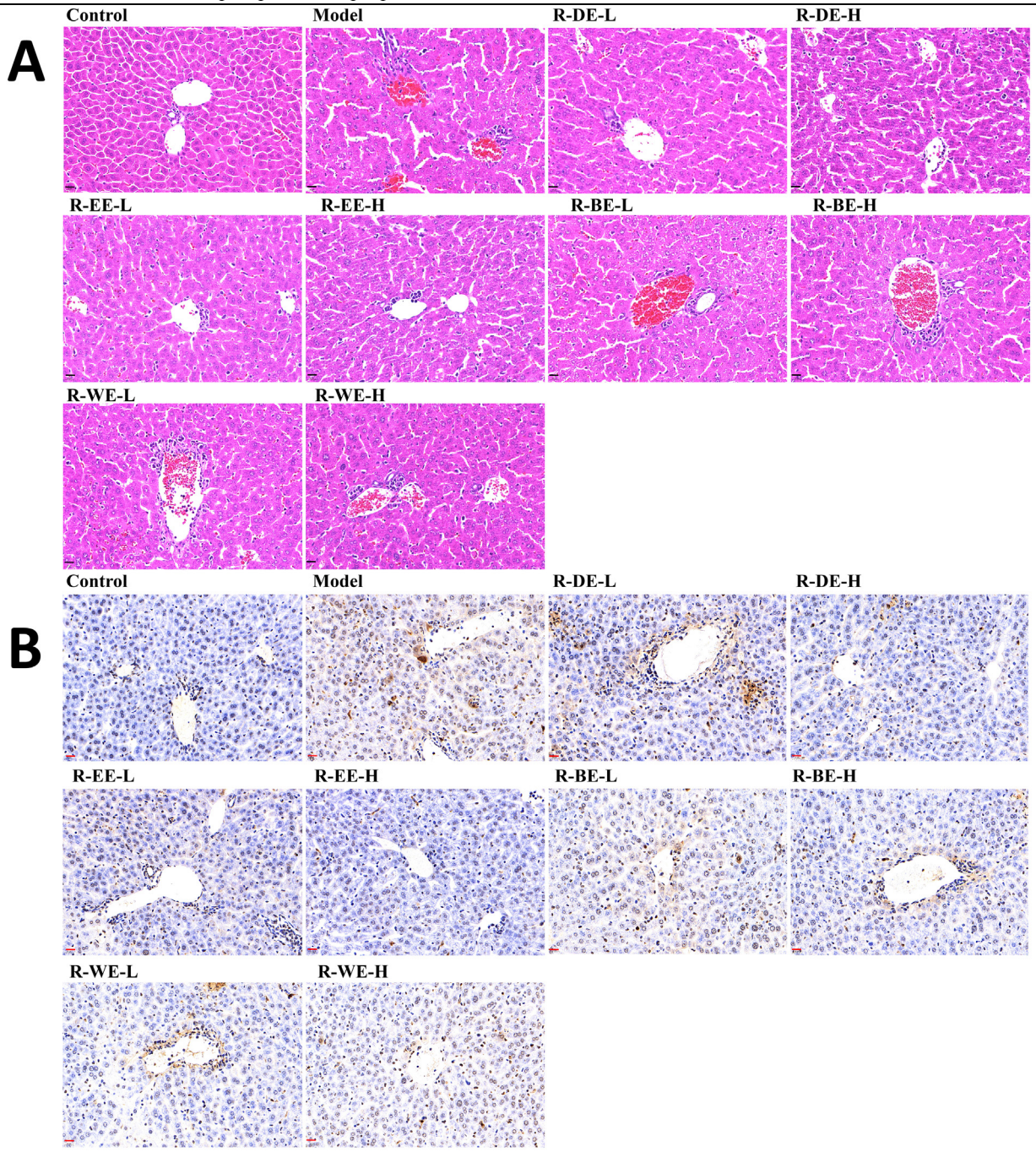
A
Control
Model
R-DE-L
R-DE-H
R-EE-L
R-EE-H
R-BE-L
R-BE-H
R-WE-L
R-WE-H
B
Control
Model
R-DE-L
R-DE-H
R-EE-L
R-EE-H
R-BE-L
R-BE-H
R-WE-L
R-WE-H

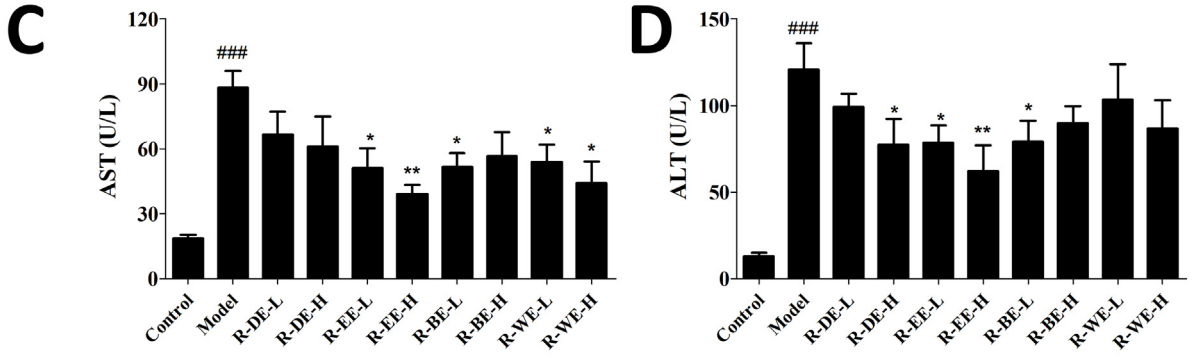
C
AST (U/L)
120
90
60
30
0
###
*
**
Control
Model
R-DE-L
R-DE-H
R-EE-L
R-EE-H
R-BE-L
R-BE-H
R-WE-L
R-WE-H
D
ALT (U/L)
150
100
50
0
###
*
**
Control
Model
R-DE-L
R-DE-H
R-EE-L
R-EE-H
R-BE-L
R-BE-H
R-WE-L
R-WE-H

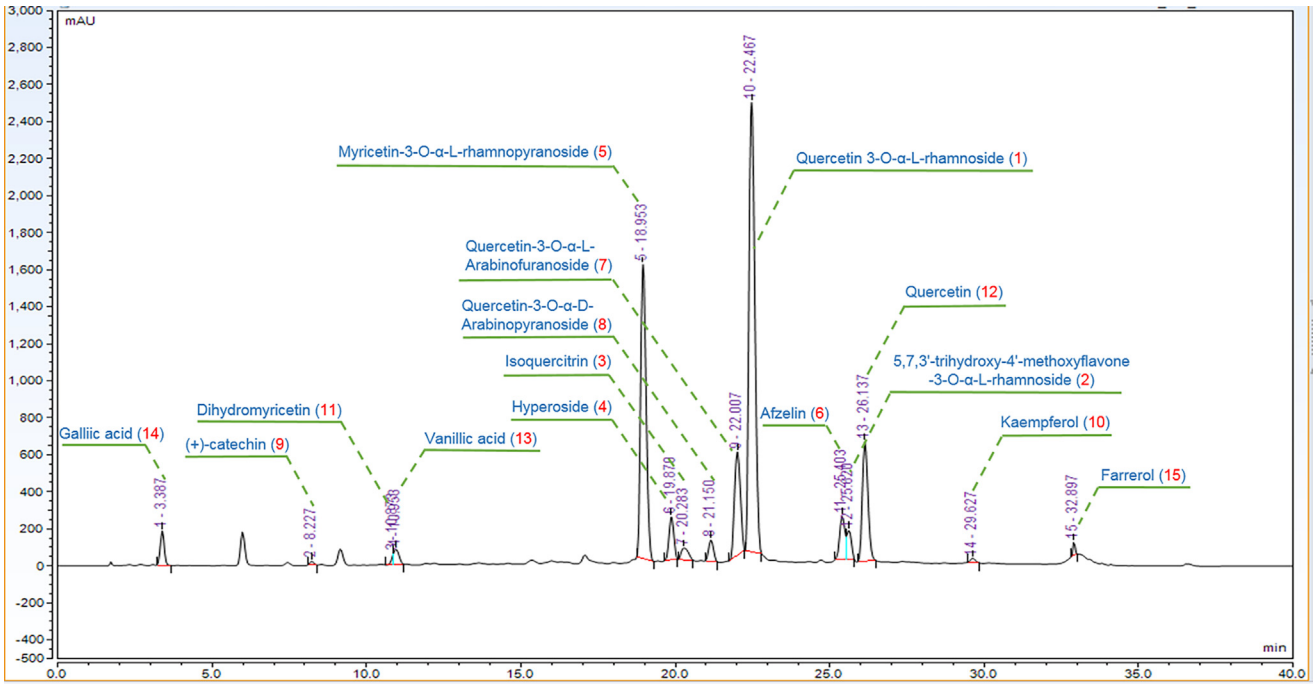

Fig. 2 HPLC chromatogram of the EtOAc extracts (REE).

that 883 GO terms were enriched, including 665 biological processes, 79 cellular components, and 139 molecular functions. We extracted the top 20 significantly enriched terms from the three categories according to the - log10 (P Value) and displayed them using bar charts in Fig. 5. Based on the GO enrichment analysis, positive regulation of gene expression (GO: 0010628), positive regulation of transcription (GO: 0045893) and inflammatory response (GO: 0006954) were significantly enriched. Furthermore, the top important signaling pathways of the KEGG results are shown in the bubble chart. The results proved that the potential targets were primarily gathered in some inflammation-associated signaling pathways, including IL17, TNF, Toll-like receptor signaling, and NF-κB. Among them, NF-κB, as the most common and important signaling pathway, has been reported to regulate multiple aspects of innate and adaptive immune functions and act as a pivotal mediator of inflammatory responses. Once activated, NF-κB translocates from the cytoplasm into the nucleus and induces the expression of various proinflammatory genes, including those encoding cytokines and chemokines. These data provide the theoretical basis that *R-EE* against AIH activity may be related to the regulation of IL17, TNF cytokines and the NF-κB signaling pathway. The results could help us to better elucidate the effect of *R-EE* against AIH.

3.5. Effect of R-EE on inflammatory cytokine production in ConA-induced hepatitis

Previous studies revealed that activation of immune cells such as Kupffer cells and T cells is critical in Con A-induced hepatitis, and subsequently associated with the secretion of inflammatory cytokines, including TNF-α, IL-6, IL-1β and IFN-γ. To investigate the influence of *R-EE* on the release of inflammatory cytokines, the cytokine levels of TNF-α, IFN-γ and IL-1β in serum as well as those genes in the liver of mice were measured by ELISA and qRT-PCR methods. As shown in Fig. 6A and B, the levels of TNF-α, IFN-γ, and IL-1β were significantly increased following ConA injection, which indicated inflammatory system disorder in ConA-induced hepatitis mice. *R-EE* treatment significantly alleviated the serum levels of TNF-α, IFN-γ and IL-1β. These data suggested that *R-EE* treatment restrained the excessive release of pro-inflammatory cytokines.

3.6. Effect of R-EE on the hepatic infiltration of $CD4^+$ T cells and inflammation in Con A-induced hepatitis

Accumulating evidence has revealed that T cells and macrophages play vital roles in Con A-induced hepatitis, especially

Fig. 1 Protective effect of *R. simsii* Planch extracts on ConA-induced AIH in mice. (**A**) Liver pathological changes examined by HE (magnification 40 ×), (**B**) Apoptosis of liver by TUNEL staining (magnification 40 ×), (**C** and **D**) Serum AST and ALT levels. L and H indicate the gavage doses of 25 and 50 mg/kg, respectively. Data (n = 6) are expressed as the mean ± SEM. $^{###}p < 0.001$, compared with normal; $^{*}p < 0.05$,** $p < 0.01$, comparing with model.

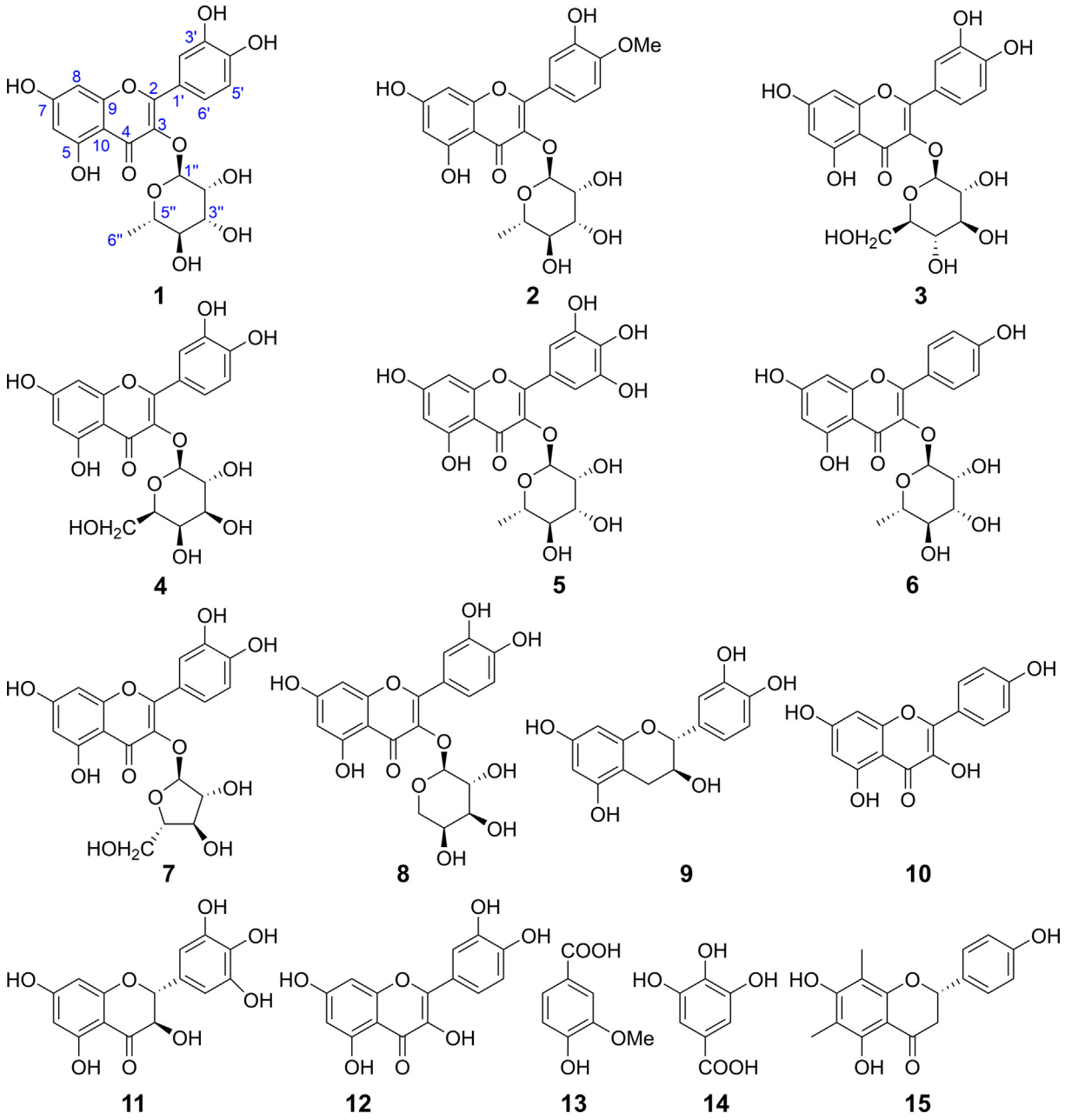

Fig. 3 Chemical structures of compounds isolated from EtOAc extract (*R-EE*).

$CD4^+$ T cells and Kupffer cells. To detect the infiltration of inflammatory cells, $CD4^+$ cells were used to examine inflammatory cell accumulation in the liver. Immunohistochemical analysis showed that the number of $CD4^+$ cells significantly increased in the liver, but slipped to basal levels by *R-EE* treatment (Fig. 6C). Meanwhile, NF-κB is also only responsible for the priming step of the NLRP3 inflammasome, thus, IHC was also conducted to test activated NLRP3 inflammasome in ConA-induced liver injury. ConA significantly elevated the levels of the NLRP3 inflammasome, and the increase was clearly inhibited by treatment with *R-EE*.

3.7. Effect of R-EE extraction on NLPR3/NF-κB signaling in Con A-induced hepatitis

It has been reported that NF-κB works as an important modulator of inflammation and the immune response and executes a major role in liver disease. As shown in Fig. 7, administration of ConA induced a significant increase in the phosphorylation of IκBα indicating the activation of NF-κB signaling, whereas *R-EE* treatment significantly attenuated the cytosolic phosphorylation of IκBα. Meanwhile, our data showed that the expres-

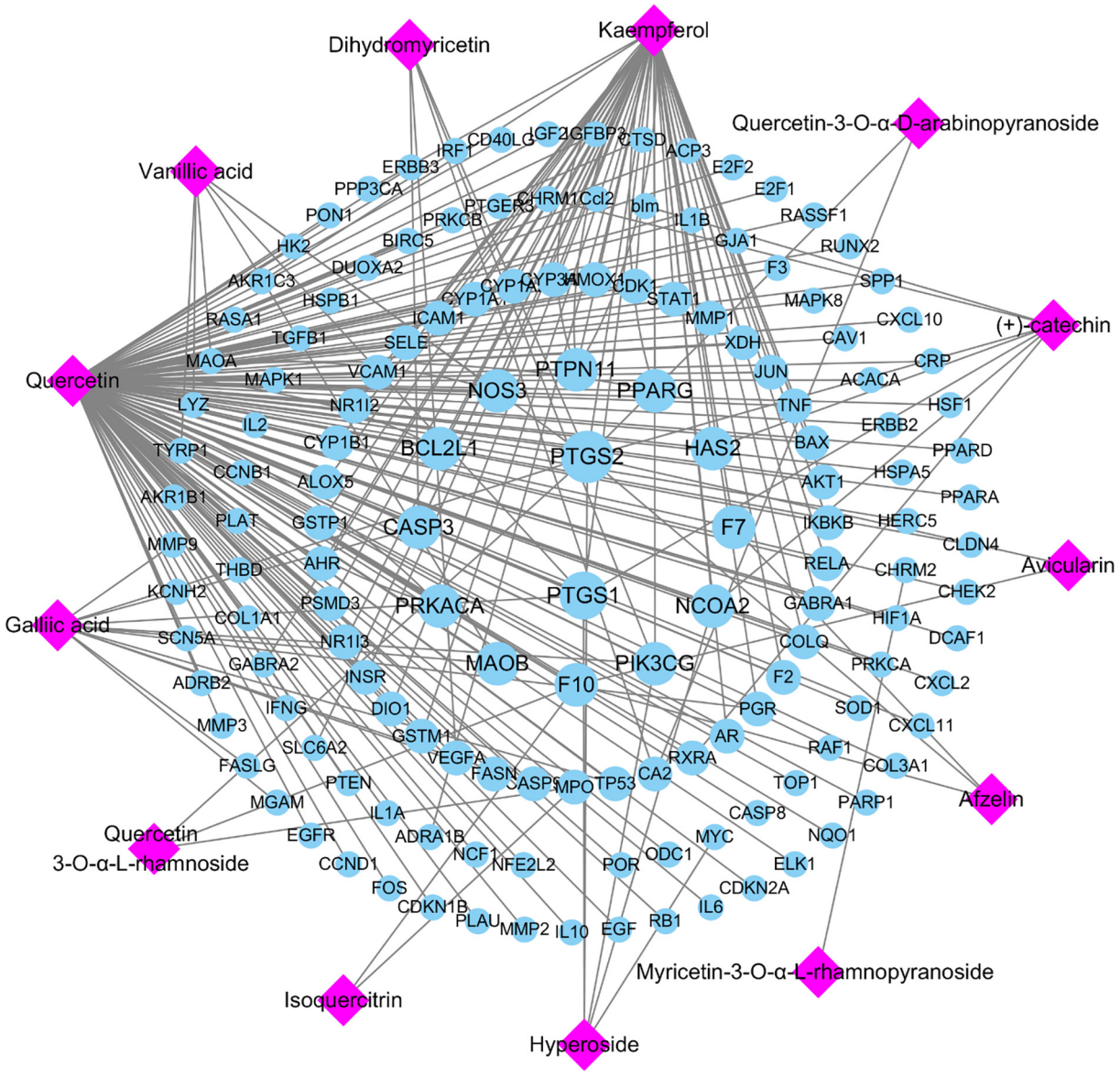

Fig. 4 Potential active ingredient-target network of *R-EE* acting on AIH-related targets.

sion of NLPR3 and COX-2 was dramatically increased in the ConA group and that treatment with *R-EE* significantly altered the increased levels, which was consistent with the immunohistochemical analysis. Thus, *R-EE*'s prevention of ConA-induced hepatitis is associated with reduced production of pro-inflammatory cytokines and chemokines in the liver *via* the NF-κB signaling pathway.

4. Discussion

Autoimmune hepatitis (AIH) is an inflammatory disease of the liver with a rising incidence each year (Hennes et al., 2008; Chinese Society of Hepatology et al., 2017). The main clinicopathological features include inflammatory cell infiltration, $CD4^+$ T-cell response to the production of IFN-γ and TNF-α (Bovensiepen et al., 2019), and hepatic necrosis, accompanied by elevation of ALT and AST (Czaja et al., 2016; Roberts et al., 2017). Untreated AIH, can lead to hepatitis, fibrosis, cirrhosis and liver failure (Krawitt et al., 2006). Anti-inflammatory drugs, immunosuppressants and liver transplantation are the current treatment options (Feng et al., 2018; Lowe et al., 2018; Liwinski et al., 2017). Unfortunately, steroids and immunosuppressive agents often have deleterious side effects that lead to intolerance, and the benefits and risks of corticosteroid therapy remain unclear (Czaja et al., 2005). Hence, new therapeutic agents are urgently needed. The ConA-induced AIH model is a classical experimental model with similar histological and serological changes to human AIH patients (Jaeckel et al., 2011), and has been commonly used in the field of liver injury research (Xu et al., 2018). Some medicinal plants of the *Rhododendron* family have been proven to be effective in analgesia, glomerulonephritis and rheumatoid arthritis (Qiu et al., 2019). *Rhododendron simsii* Planch is used as a folk medicine to treat various inflammatory and immune-related diseases in China. (Nanjing University of Traditional Chinese Medicine, 2006). Previous phytochemical

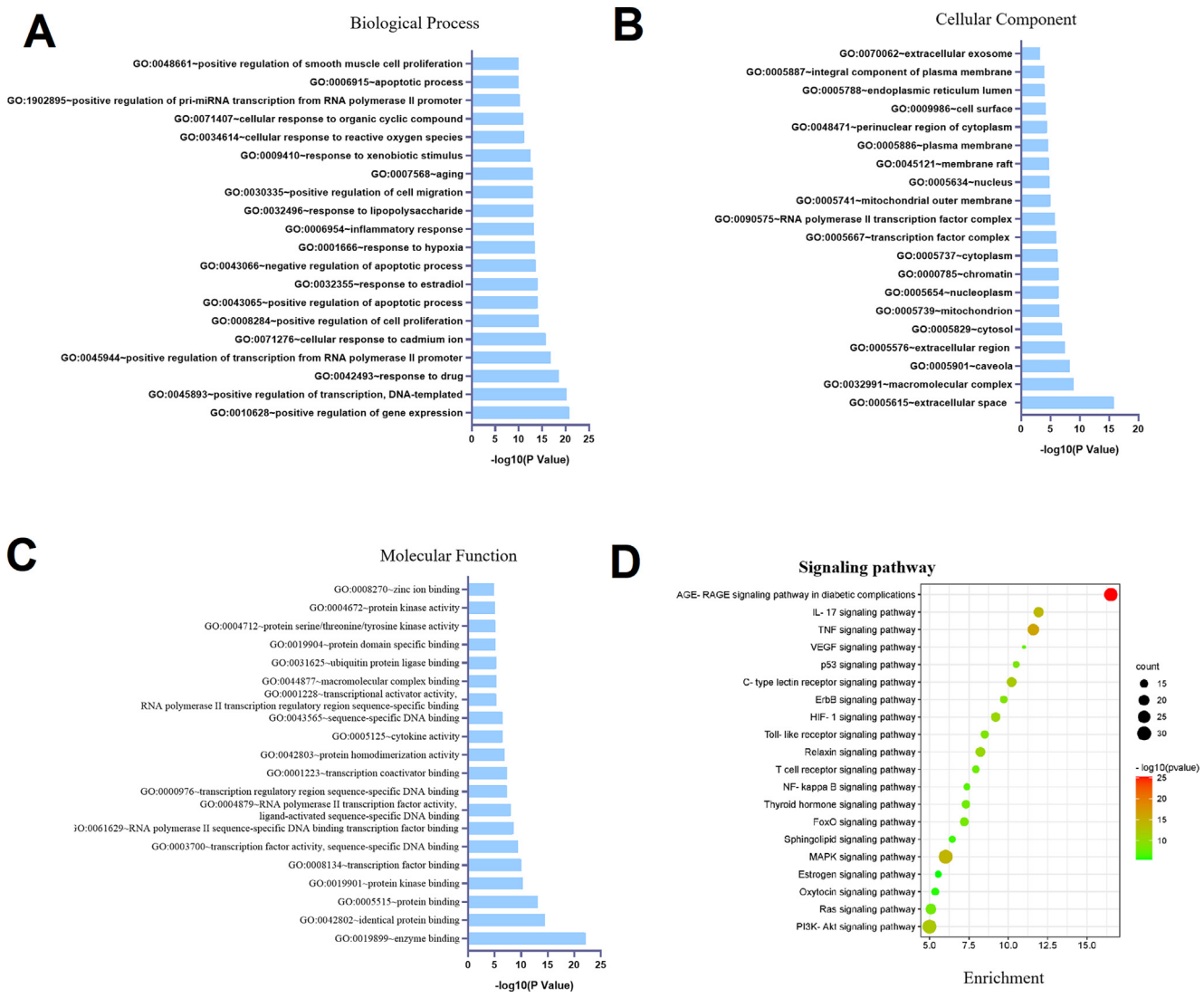

Fig. 5 Dot plot of the top 20 functional enrichment results. (**A**) Biological process. (**B**) Molecular function. (**C**) Cellular component. (**D**) KEGG signaling pathway.

investigations have shown that majority of the characterized components in *Ericaceae* are flavonoids, triterpenes, diterpenes, lignans and other derivatives (Wang et al., 2014), and there is no report of *R. simsii* Planch against AIH. Based on the literature analysis, UV absorption at 254 nm, and color spot on TLC under $FeCl_3$ (dark green) or 5% H_2SO_4 (pink or red) reagent, *R-DE* contains terpenoids, *R-BE* contains flavonoid glycosides and phenols, and *R-WE* contains carbohydrates, while the main components of *R-BE* are flavonoids, and the structures were identified as quercetin 3-O-α-L-rhamnoside (1) (Wang, Y.F. et al., 2020), tamarixetin 3-rhamnoside (2) (Son et al., 2005; He et al., 2001), isoquercitrin (3) (Takeda et al., 2001), hyperoside (4) (Wu et al., 2012; Wu et al., 2010), myricetin-3-O-α-L-rhamnopyranoside (5) (Zeng et al., 2013), afzelin (6) (Wang et al., 2007), quercetin-3-O-α-L-arabinofuranoside (7) (Kim et al., 1994), quercetin-3-O-α-D-arabinopyranoside (8) (Liu et al., 2009), (+)-catechin (9) (Khalid et al., 1989; Zhou et al., 2000), kaempferol (10) (Wang, L. et al., 2020), dihydromyricetin (11) (Jin et al., 2009), quercetin (12) (Fossen et al., 1998), vanillic acid (13) (Gutierrez-Lugo et al., 2005), gallic acid (14) (Deng and Qin, 2008), farrerol (15) (Li et al., 2014) respectively, based on isolation, purification and NMR spectral analysis. Here, we used ConA induced autoimmune hepatitis to explore the protective effects as well as the potential mechanisms of *Rhododendron simsii* Planch on autoimmune hepatitis.

A single injection of ConA can lead to activation and differentiation of T cells, particularly $CD4^+$ T cells in liver tissue (Tiegs et al., 1992). ConA has a high affinity toward MHC class II, mannose receptor (MR), and intracellular adhesion molecule-1 (ICMA-1) on sinusoid endothelial cells (SECs), and leads to the breakdown of the membrane, releasing the MHC class II-Con A complex, which promotes the adhesion of ConA to Kupffer cells (KCs) (Wang et al., 2012). The complex activates Th0 cells to differentiate into Th1, Th2, Th17, and regulatory T cells (Tregs) by recognizing T-cell receptors (TCRs), Th1 and Th17 cells secrete tumor necrosis factor TNF-α, interferon IFN-γ, interleukin IL-17, and IL-22, which

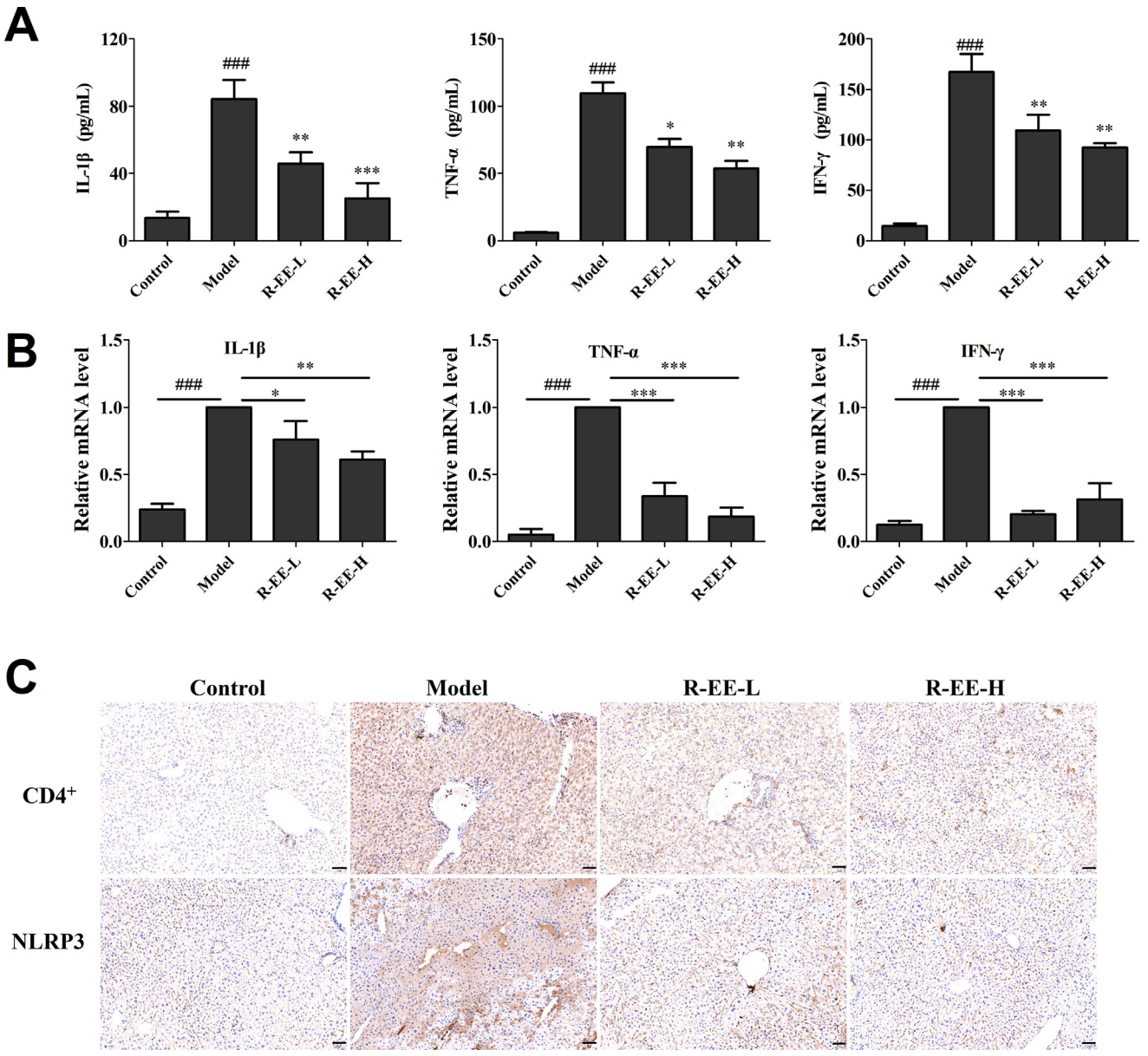

Fig. 6 Effects of *R-EE* on Con A-induced hepatitis. (**A**) Secretions of IL-1β TNF-α, and IFN-γ in serum (ELISA), (**B**) mRNA expression of IL-1β TNF-α, and IFN-γ (qRT-PCR), (**C** and **D**) Expression of $CD4^+$ and NLRP3 (examined by IHC, magnification 20 ×). Data (n = 6) are expressed as the mean ± SEM. $^{\#\#\#}p < 0.001$, compared with normal; *p < 0.05, ** p < 0.01, *** p < 0.001, compared with model.

can induce hepatocyte apoptosis and necrosis (Webb et al., 2018). ConA can also activate macrophages and neutrophils via MRs, to induce the synthesis of cytokines such as TNF-α, IFN-γ, IL-1β and ROS (Strasser et al., 2009). Meanwhile, in the ConA induced hepatitis model, there was a marked increase in the serum markers of ALP, AST and ALT, which are released into the blood after hepatocyte injury (Liu et al., 2019; Tian et al., 2019). Our current study revealed that *R-EE* treatment prevented microscopic disruptions, hepatocyte necrosis and apoptosis, accompanied by a reduction in ALT and AST. In subsequent experiments, we found that *R-EE* can significantly alleviate the levels of TNF-α, IFN-γ and IL-1β; meanwhile, immunohistochemical analysis showed that the number of $CD4^+$ cells slipped to basal levels after treatment in ConA-induced hepatitis mice. These results indicated that *R-EE* exhibits hepatoprotective effects by reversing the disorder of the inflammatory system in Con A hepatitis mice.

NF-κB plays a pivotal role in establishing the Con A-induced hepatitis model. It is the intersection of numerous signaling pathways, and is also associated with the release and expression of downstream cytokines (Xue et al., 2015; El-Agamy et al., 2016) Proinflammatory cytokines, including TNF-α and IL-1β produced by Th cells, macrophages and neutrophils in the ConA-induced hepatitis model, result in activation of the inhibitory κB kinase (IKK) complex, and NF-κB dimers translocate to the nucleus, ultimately leading to the

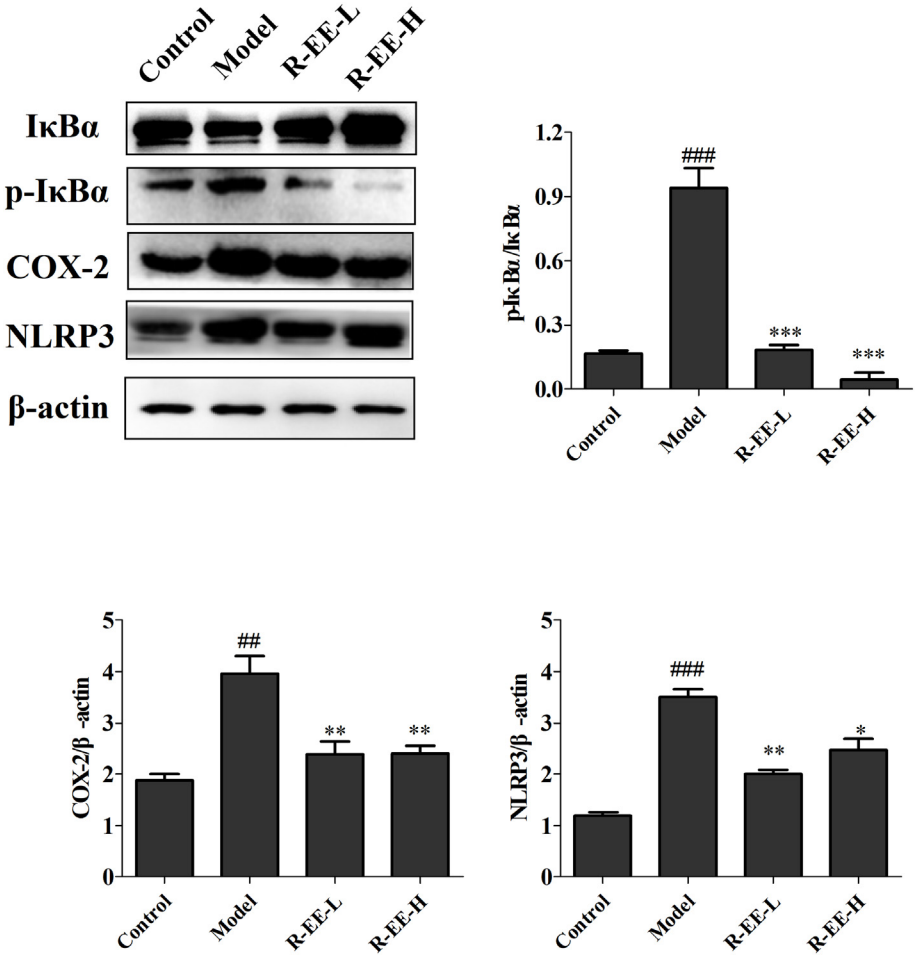

Fig. 7 Protein expression of IκBα, p-IκBα, COX-2, and NLRP3 ConA-induced hepatitis treated with *R-EE* (n = 3). $^{\#\#}p < 0.01$, $^{\#\#\#}p < 0.001$, compared with normal; *p < 0.05, **p < 0.01, significant difference vs. model.

expression of multiple inflammatory and immune genes. (Liu et al., 2022). Activation of the NLRP3 (Nod-like receptor 3) inflammasome results in shortened survival, poor growth, and severe hepatic inflammatory responses characterized by neutrophil infiltration, hepatic stellate cell (HSC) activation, and collagen deposition (Wree et al., 2014). It is also involved in the intensification of inflammatory responses through the activation of precaspase-1 and release of IL-1β and IL − 18 (Ibrahim et al., 2021). Previous studies suggested a direct link between COX-2 and hepatitis (Holt et al., 2007). COX-2 is markedly increased in cirrhosis and chronic hepatitis (Mohammed et al., 2004). Inhibition of COX-2 can reduce the severity of hepatitis (Yu et al., 2006). Our results revealed that the administration of *R-EE* attenuated the activation of NF-κB, and reduced COX-2, and NLRP3 expression, which may be the potential mechanism for the hepatoprotective effect.

5. Conclusions

Our study confirms the rationality of traditional application of *Rhododendron simsii* Planch in the treatment of inflammatory diseases, and provides evidence for the hepatoprotective effect of *R-EE* in Con A-induced hepatitis. *R-EE* could reduce ConA-induced hepatocyte congestion, lymphocyte infiltration and necrosis, and reduce serum ALT and AST levels, down-regulate the $CD4^+$ cells, inflammatory cytokines levels and expressions of NLPR3, COX-2 and p-IκBα, which may be related to its considerable flavonoids and phenolic derivatives. The potential mechanism was associated with the reduced release of inflammatory factors, expression of $CD4^+$ cells and regulation of the NF-κB signaling pathway. *R-EE* is a potential treatment agent for AIH that deserves further study.

CRediT authorship contribution statement

Fuqian Wang: Investigation, Validation, Writing – original draft. **Weiguang Sun:** Validation, Supervision. **Zhou Lan:** Validation, Supervision. **Yuan Zhou:** Supervision. **Lulu Li:** . **Ziheng Li:** Validation, Supervision. **Ling Cheng:** Supervision. **Qiuyun You:** Supervision. **Qunfeng Yao:** Supervision.

Declaration of Competing Interest

The authors declare that they have no known competing financial interests or personal relationships that could have appeared to influence the work reported in this paper.

Acknowledgments

This work was supported by Scientific Research Project of Wuhan Municipal Health Commission (WX20A14).

Chemical compounds from *Rhododendron simsii* Planch in this manuscript

Quercetin 3-O-α-L-rhamnoside (CAS: 522-12-3), tamarixetin 3-rhamnoside (CAS: 87562-18-3), isoquercitrin (CAS: 482-35-9), hyperoside (CAS: 482-36-0), myricetin-3-O-α-L-rhamnopyranoside (CAS: 17912-87-7), afzelin (CAS: 482-39-3), quercetin-3-O-α-L-arabinofuranoside (CAS: 572-30-5), quercetin-3-O-α-D-arabinopyranoside (CAS: 6743-88-0), (+)-catechin (CAS: 154-23-4), kaempferol (CAS: 520-18-3), dihydromyricetin (CAS: 27200-12-0), quercetin (CAS: 117-39-5), vanillic acid (CAS: 121-34-6), gallic acid (CAS: 149-91-7) and farrerol (CAS: 24211-30-1)

Appendix A. Supplementary material

Supplementary data to this article can be found online at https://doi.org/10.1016/j.arabjc.2023.104955.

References

Bovensiepen, C.S., Schakat, M., Sebode, M., Zenouzi, R., Hartl, J., Peiseler, M., Li, J., Henze, L., Woestemeier, A., Schramm, C., Lohse, A.W., Herkel, J., Weiler-Normann, C., 2019. TNF-producing Th1 cells are selectively expanded in liver infiltrates of patients with autoimmune hepatitis. J. Immunol. 203, 3148–3156. https://doi.org/10.4049/jimmunol.1900124.

Carta, S., Penco, F., Lavieri, R., Martini, A., Dinarello, C.A., Gattorno, M., Rubartelli, A., 2015. Cell stress increases ATP release in NLRP3 inflammasome-mediated autoinflammatory diseases, resulting in cytokine imbalance. Proc. Natl. Acad. Sci. USA 112, 2835–2840. https://doi.org/10.1073/pnas.1424741112.

Chinese Herbal Medicine Research Group, Training Department, Second Military Medical University, 1978. Studies on the active constituents of *Rhododendron simsii* Planch. Chinese Pharmaceutical Journal. 1, 30

Chinese Society of Hepatology, Chinese Society of Gastroenterology & Chinese Society of Infectious Diseases., 2017. Chinese consensus on the diagnosis and management of autoimmune hepatitis (2015). J Dig Dis. 18, 247–264. https://doi.org/10.1111/1751-2980.12479

Czaja, A.J., 2016. Nature and implications of oxidative and nitrosative stresses in autoimmune hepatitis. Dig. Dis. Sci. 61, 2784–2803. https://doi.org/10.1007/s10620-016-4247-6.

Czaja, A.J., Bianchi, F.B., Carpenter, H.A., Krawitt, E.L., Lohse, A. W., Manns, M.P., McFarlane, I.G., Mieli-Vergani, G., Toda, G., Vergani, D., Vierling, J., Zeniya, M., 2005. Treatment challenges and investigational opportunities in autoimmune hepatitis. Hepatology 41, 207–215. https://doi.org/10.1002/hep.20539.

Deng, A.J., Qin, H.L., 2008. Studies on chemical constituents of fruits of *Bridelia tomentosa*. China J. Chinese Mater. Med. 33, 158–160.

El-Agamy, D.S., 2016. Pirfenidone ameliorates concanavalin A-induced hepatitis in mice via modulation of reactive oxygen species/nuclear factor kappa B signalling pathways. J. Pharm. Pharmacol. 68, 1559–1566. https://doi.org/10.1111/jphp.12651.

Feng, J., Niu, P., Chen, K., Wu, L., Liu, T., Xu, S., Li, J., Li, S., Wang, W., Lu, X., Yu, Q., Liu, N., Xu, L., Wang, F., Dai, W., Xia, Y., Fan, X., Guo, C., 2018. Salidroside mediates apoptosis and autophagy inhibition in concanavalin A-induced liver injury. Exp. Ther. Med. 15, 4599–4614. https://doi.org/10.3892/etm.2018.6053.

Ferri, S., Longhi, M.S., De Molo, C., Lalanne, C., Muratori, P., Granito, A., Hussain, M.J., Ma, Y., Lenzi, M., Mieli-Vergani, G., Bianchi, F.B., Vergani, D., Muratori, L., 2010. A multifaceted imbalance of T cells with regulatory function characterizes type 1 autoimmune hepatitis. Hepatology 52, 999–1007. https://doi.org/10.1002/hep.23792.

Fossen, T., Pedersen, A.T., Andersen, Ø.M., 1998. Flavonoids from red onion (*Allium cepa*). Phytochemistry 47, 281–285. https://doi.org/10.1016/S0031-9422(97)00423-8.

Guo, Y., Yu, X.M., Chen, S., Wen, J.Y., Chen, Z.W., 2020. Total flavones of *Rhododendron simsii* Planch flower protect rat hippocampal neuron from hypoxia-reoxygenation injury via activation of BKCa channel. J. Pharm. Pharmacol. 72, 111–120. https://doi.org/10.1111/jphp.13178.

Gutierrez-Lugo, M.T., Woldemichael, G.M., Singh, M.P., Suarez, P. A., Maiese, W.M., Montenegro, G., Timmermann, B.N., 2005. Isolation of three new naturally occurring compounds from the culture of *Micromonospora* sp. P1068. Nat. Prod. Res. 19, 645–652. https://doi.org/10.1080/14786410412331272040.

He, H.P., Zhu, W.M., Shen, Y.M., Yang, X.S., Zuo, G., Hao, X., 2001. Flavonoid glycosides from Clausena excavata (in Chinese). Acta Botanica Yunnanica, 2001, 23(2): 256–260.

Hennes, E.M., Zeniya, M., Czaja, A.J., Parés, A., Dalekos, G.N., Krawitt, E.L., Bittencourt, P.L., Porta, G., Boberg, K.M., Hofer, H., Bianchi, F.B., Shibata, M., Schramm, C., Eisenmann de Torres, B., Galle, P.R., McFarlane, I., Dienes, H.P., Lohse, A.W., 2008. International autoimmune hepatitis group. simplified criteria for the diagnosis of autoimmune hepatitis. Hepatology 48, 169–176. https://doi.org/10.1002/hep.22322.

Herkel, J., Carambia, A., Lohse, A.W., 2020. Autoimmune hepatitis: possible triggers, potential treatments. J. Hepatol. 73, 446–448. https://doi.org/10.1016/j.jhep.2020.03.015.

Heymann, F., Hamesch, K., Weiskirchen, R., Tacke, F., 2015. The concanavalin A model of acute hepatitis in mice. Lab. Anim. 49, 12–20. https://doi.org/10.1177/0023677215572841.

Holt, A.P., Adams, D.H., 2007. Complex roles of cyclo-oxygenase 2 in hepatitis. Gut 56, 903–904. https://doi.org/10.1136/gut.2006.115972.

Huang, G.H., Hu, Z., Lei, C., Wang, P.P., Yang, J., Li, J.Y., Li, J., Hou, A.J., 2018. Enantiomeric pairs of meroterpenoids with diverse heterocyclic systems from *Rhododendron nyingchiense*. J. Nat. Prod. 81, 1810–1818. https://doi.org/10.1021/acs.jnatprod.8b00273.

Huang, Y., Xu, W., Zhou, R., 2021. NLRP3 inflammasome activation and cell death. Cell. Mol. Immunol. 18, 2114–2127. https://doi.org/10.1038/s41423-021-00740-6.

Ibrahim, S.R.M., Sirwi, A., Eid, B.G., Mohamed, S.G.A., Mohamed, G.A., 2021. Summary of natural products ameliorate concanavalin A-induced liver injury: structures, sources, pharmacological effects, and mechanisms of action. Plants (Basel) 10, 228. https://doi.org/10.3390/plants10020228.

Jaeckel, E., Hardtke-Wolenski, M., Fischer, K., 2011. The benefit of animal models for autoimmune hepatitis. Best Pract. Res. Clin. Gastroenterol. 25, 643–651. https://doi.org/10.1016/j.bpg.2011.10.006.

Jiang, R., Tang, J., Zhang, X., He, Y., Yu, Z., Chen, S., Xia, J., Lin, J., Ou, Q., 2022. CCN1 Promotes inflammation by inducing IL-6 production via α6β1/PI3K/Akt/NF-κB pathway in autoimmune hepatitis. Front. Immunol. 13,. https://doi.org/10.3389/fimmu.2022.810671 810671.

Jin, H.Z., Chen, G., Li, X.F., Shen, Y.H., Yan, S.K., Zhang, L., Yang, M., Zhang, W.D., 2009. Flavonoids from *Rhododendron decorum*. Chem. Nat. Compd. 45, 85–86. https://doi.org/10.1007/s10600-009-9245-x.

Khalid, S.A., Yagi, S.M., Khristova, P., Duddeck, H., 1989. (+)-Catechin-5-galloyl ester as a novel natural polyphenol from the bark of *Acacia nilotica* of sudanese origin1. Planta Med. 55, 556–558. https://doi.org/10.1055/s-2006-962094.

Kim, H.J., Woo, E.R., Park, H., 1994. A novel lignan and flavonoids from Polygonum aviculare. J. Nat. Prod. 57 (5), 581–586. https://doi.org/10.1021/np50107a003.

Komori, A., 2021. Recent updates on the management of autoimmune hepatitis. Clin. Mol. Hepatol. 27, 58–69. https://doi.org/10.3350/cmh.2020.0189.

Krawitt, E.L., 2006. Autoimmune hepatitis. N. Engl. J. Med. 354, 54–66. https://doi.org/10.1056/NEJMra050408.

Li, Y., Liu, Y.B., Yu, S.S., 2013. Grayanoids from the *Ericaceae* family: structures, biological activities and mechanism of action. Phytochem. Rev 12, 305–325. https://doi.org/10.1007/s11101-013-9299-z.

Li, G.P., Luo, Y., Li, S.X., Yang, C., Tian, Q., Zuo, M.Y., 2014. Chemical constituents in flowers of *Rhododendron lapponicum*. Chinese Trad. Herb. Drugs 45, 1668–1672. https://doi.org/10.7501/j.issn.0253-2670.2014.12.002.

Liu, Y., Hao, H., Hou, T., 2022. Concanavalin A-induced autoimmune hepatitis model in mice: mechanisms and future outlook. Open Life Sci. 17, 91–101. https://doi.org/10.1515/biol-2022-0013.

Liu, J., Mao, Y.D., 2019. Eugenol attenuates concanavalin A-induced hepatitis through modulation of cytokine levels and inhibition of mitochondrial oxidative stress. Arch. Biol. Sci. 71, 339–346. https://doi.org/10.2298/ABS190121016L.

Liu, F., Wang, Y.N., Li, Y., Ma, S.G., Qu, J., Liu, Y.B., Niu, C.S., Tang, Z.H., Li, Y.H., Li, L., Yu, S.S., 2018. Minor nortriterpenoids from the twigs and leaves of *Rhododendron latoucheae*. J. Nat. Prod. 81, 1721–1733. https://doi.org/10.1021/acs.jnatprod.7b01074.

Liu, J.S., Xiong, J., Zhu, Z.H., Li, Z.Q., Zhu, H.Y., Deng, A.G., 2005. Modulation of *Rhododendron molle* root extract on NFκB expression in chronic glomerular nephritis (in Chinese). Chin. J. Nephrol. 21, 696–697.

Liu, H., Xu, L., Peng, Y., Li, R., Xiao, P., 2009. Chemical study on ethyl acetate soluble portion of *Kadsura oblongifolia*. China J. Chinese Mater. Med. 34, 864–866. PMID: 19623983.

Liwinski, T., Schramm, C., 2017. Autoimmune hepatitis - update on clinical management in 2017. Clin. Res. Hepatol. Gastroenterol. 41, 617–625. https://doi.org/10.1016/j.clinre.2017.07.002.

Lowe, D., John, S., 2018. Autoimmune hepatitis: appraisal of current treatment guidelines. World J. Hepatol. 10, 911–923. https://doi.org/10.4254/wjh.v10.i12.911.

Luo, Y.Y., Zha, J.Q., Li, Y.Q., Li, Y.L., Zeng, F.B., 1993. Retrospective study on roots of *Rododendron molle* in the treatment of rheumatoid arthritis in 114 cases (in Chinese). Chin. J. Integr. Tradit. West. Med. 13, 489–490.

Ma, H.D., Deng, Y.R., Tian, Z., Lian, Z.X., 2013. Traditional Chinese medicine and immune regulation. Clin. Rev. Allerg. Immunol. 44, 229–241. https://doi.org/10.1007/s12016-012-8332-0.

Mieli-Vergani, G., Vergani, D., Czaja, A.J., Manns, M.P., Krawitt, E. L., Vierling, J.M., Lohse, A.W., Montano-Loza, A.J., 2018. Autoimmune hepatitis. Nat. Rev. Dis. Primers 4, 18017. https://doi.org/10.1038/nrdp.2018.17.

Mohammed, N.A., Abd El-Aleem, S.A., El-Hafiz, H.A., McMahon, R.F., 2004. Distribution of constitutive (COX-1) and inducible (COX-2) cyclooxygenase in postviral human liver cirrhosis: a possible role for COX-2 in the pathogenesis of liver cirrhosis. J. Clin. Pathol. 57, 350–354. https://doi.org/10.1136/jcp.2003.012120.

Nanjing University of Traditional Chinese Medicine, 2006. Dictionary of Chinese Materia Medica. Shanghai Scientific & Technical Publishers, Shanghai, pp. 1520–1522

Popescu, R., Kopp, B., 2013. The genus Rhododendron: an ethnopharmacological and toxicological review. J. Ethnopharmacol. 147, 42–62. https://doi.org/10.1016/j.jep.2013.02.022.

Qiu, Y., Zhou, J., Zhang, H., Zhou, H., Tang, H., Lei, C., Ye, C., You, C., Chen, Y., Wang, Y., Xiong, J., Su, H., Yao, G., Zhang, C., 2019. Rhodojaponin II attenuates kidney injury by regulating TGF-β1/Smad pathway in mice with adriamycin nephropathy. J. Ethnopharmacol. 243,. https://doi.org/10.1016/j.jep.2019.112078 112078.

Roberts, S.K., Kemp, W., 2017. Salvage therapies for autoimmune hepatitis: a critical review. Semin. Liver Dis. 37, 343–362. https://doi.org/10.1055/s-0037-1607453.

Ru, J., Li, P., Wang, J., Zhou, W., Li, B., Huang, C., Li, P., Guo, Z., Tao, W., Yang, Y., Xu, X., Li, Y., Wang, Y., Yang, L., 2014. TCMSP: a database of systems pharmacology for drug discovery from herbal medicines. J. Cheminform. 6, 13. https://doi.org/10.1186/1758-2946-6-13.

Safran, M., Chalifa-Caspi, V., Shmueli, O., Olende,r T., Lapidot, M., Rosen, N., Shmoish, M., Peter, Y., Glusman, G., Feldmesser, E., Adato, A., Peter, I., Khen, M., Atarot, T., Groner, Y., Lancet, D., 2003. Human gene-centric databases at the weizmann institute of science: genecards, UDB, CroW 21 and HORDE. Nucleic Acids Res. 31, 142–146. https://doi.org/10.1093/nar/gkg050.

Sebode, M., Schulz, L., Lohse, A.W., 2017. "Autoimmune(-Like)" drug and herb induced liver injury: new insights into molecular pathogenesis. Int. J. Mol. Sci. 18, 1954. https://doi.org/10.3390/ijms18091954.

Son, Y.K., Lee, M.H., Han, Y.N., 2005. A new antipsychotic effective neolignan from *Firmiana simplex*. Arch. Pharm. Res. 28, 34–38. https://doi.org/10.1007/BF02975132.

Song, X.P., Chen, Z.W., Zhang, J.H., 2006. Analgesic effects of total flavone of *Rhododendron*. Acta Univ. Med. Anhui 41, 427–430. https://doi.org/10.19405/j.cnki.issn1000-1492.2006.04.021.

Song, X.P., Chen, Z.W., Zhang, J.H., Ding, B., 2007. The analgesic mechanism of tatal flavone of *Rhodoendron*. J. Chinese Med. Mater. 30, 182–185. https://doi.org/10.13863/j.issn1001-4454.2007.02.025.

Strasser, A., Jost, P.J., Nagata, S., 2009. The many roles of FAS receptor signaling in the immune system. Immunity 30, 180–192. https://doi.org/10.1016/j.immuni.2009.01.001.

Sun, X.Q., Chen, S., Wang, L.F., Chen, Z.W., 2018. Total flavones of *Rhododendron simsii* Planch flower protect isolated rat heart from ischaemia-reperfusion injury and its mechanism of UTR-RhoA-ROCK pathway inhibition. J. Pharm. Pharmacol. 70, 1713–1722. https://doi.org/10.1111/jphp.13016.

Sun, L., Ma, W., Gao, W., Xing, Y., Chen, L., Xia, Z., Zhang, Z., Dai, Z., 2019. Propofol directly induces caspase-1-dependent macrophage pyroptosis through the NLRP3-ASC inflammasome. Cell Death Dis. 10, 542. https://doi.org/10.1038/s41419-019-1761-4.

Takeda, Y., Isai, N., Masuda, T., Honda, G., Takaishi, Y., Ito, M., Otsuka, H., Ashurmetov, O.A., Khodzhimatov, O.K., 2001. Phlomisflavosides A and B, new flavonol bisglycosides from *Phlomis spinidens*. Chem. Pharm. Bull. 49, 1039–1041. https://doi.org/10.1248/cpb.49.1039.

Tian, X., Liu, Y., Liu, X., Gao, S., Sun, X., 2019. Glycyrrhizic acid ammonium salt alleviates Concanavalin A-induced immunological liver injury in mice through the regulation of the balance of immune cells and the inhibition of hepatocyte apoptosis. Biomed. Pharmacother. 120,. https://doi.org/10.1016/j.biopha.2019.109481 109481.

Tiegs, G., Hentschel, J., Wende,l A., 1992. A T cell-dependent experimental liver injury in mice inducible by concanavalin A. J Clin Invest. 90, 196–203. https://doi.org/10.1172/JCI115836

Wang, M.J., 2006. Study on antitussive, asthmatic effects and toxicity of total flavones of *Rhododendra simsii* Planch. Lishizhen Medi. Mater. Med. Res. 17, 1678–1679.

Wang, Y., Chen, S., Du, K., Liang, C., Wang, S., Owusu Boadi, E., Li, J., Pang, X., He, J., Chang, Y.X., 2021. Traditional herbal medicine: Therapeutic potential in rheumatoid arthritis. J. Ethnopharmacol. 279,. https://doi.org/10.1016/j.jep.2021.114368 114368.

Wang, Y.F, Zhang, Z.X., He, R,J., Yang B,Y., Wang, L., Huang, Y. L., 2020. Study on the chemical constituents of the aerial parts of Polygonatum sibiricum and its pancreatic lipase inhibitory activity. Natural Product Research and Development, 2020, 32 (11): 1811–1817. https://doi.org/10.16333/j.1001-6880.2020.11.002.

Wang, X., Jiang, R., Liu, Z., Liu, W., Xie, M., Wei, S., She, G., 2014. Phytochemicals and biological activities of poisonous genera of *Ericaceae* in China. Nat. Prod. Commun. 9, 427–442. https://doi.org/10.1177/1934578X1400900333.

Wang, L., Li, H.Y., Liang, N., Chen, N.H., 2020. Isolation and identification of the flavonoids constituents from *Dryopteris*

championii. Nat. Prod. Res. Develop. 32, 778–782. https://doi.org/10.16333/j.1001-6880.2020.5.008.

Wang, H.X., Liu, M., Weng, S.Y., Li, J.J., Xie, C., He, H.L., Guan, W., Yuan, Y.S., Gao, J., 2012. Immune mechanisms of Concanavalin A model of autoimmune hepatitis. World J. Gastroenterol. 18, 119–125. https://doi.org/10.3748/wjg.v18.i2.119.

Wang, G.J., Tsai, T.H., Lin, L.C., 2007. Prenylflavonol, acylated flavonol glycosides and related compounds from *Epimedium sagittatum*. Phytochemistry 68, 2455–2464. https://doi.org/10.1016/j.phytochem.2007.05.035.

Webb, G.J., Hirschfield, G.M., Krawitt, E.L., 2018. Gershwin, M.E., Cellular and molecular mechanisms of autoimmune hepatitis. Annu Rev Pathol. 13, 247–292. https://doi.org/10.1146/annurev-pathol-020117-043534

Wree, A., Eguchi, A., McGeough, M.D., Pena, C.A., Johnson, C.D., Canbay, A., Hoffman, H.M., Feldstein, A.E., 2014. NLRP3 inflammasome activation results in hepatocyte pyroptosis, liver inflammation, and fibrosis in mice. Hepatology 59, 898–910. https://doi.org/10.1002/hep.26592.

Wu, Y., Ma, R., Long, C., Shu, Y., He, P., Zhou, Y., Xiang, Y., Wang, Y., 2021. The protective effect of cannabinoid type II receptor agonist AM1241 on ConA-induced liver injury in mice via mitogen-activated protein kinase signalling pathway. Int J Immunopathol Pharmacol. 35, 20587384211035251. https://doi.org/10.1177/20587384211035251.

Wu, B., Lin, W.H., 2010. Studies on chemical constituents of *Epiphyllum oxypetalum* (in Chinese). Chinese Pharma. J. 45, 496–499.

Wu, Y.B., Zheng, L.J., Wu, J.G., Chen, T.Q., Yi, J., Wu, J.Z., 2012. Antioxidant activities of extract and fractions from *Receptaculum nelumbinis* and related flavonol glycosides. Int. J. Mol. Sci. 13, 7163–7173. https://doi.org/10.3390/ijms13067163.

Xu, C., Zhang, C., Ji, J., Wang, C., Yang, J., Geng, B., Zhao, T., Zhou, H., Mu, X., Pan, J., Hu, S., Lv, Y., Chen, X., Wen, H., You, Q., 2018. CD36 deficiency attenuates immune-mediated hepatitis in mice by modulating the proapoptotic effects of CXC chemokine ligand 10. Hepatology 67, 1943–1955. https://doi.org/10.1002/hep.29716.

Xue, J., Chen, F., Wang, J., Wu, S., Zheng, M., Zhu, H., Liu, Y., He, J., Chen, Z., 2015. Emodin protects against concanavalin A-induced hepatitis in mice through inhibiting activation of the p38 MAPK-NF-κB signaling pathway. Cell. Physiol. Biochem. 35, 1557–1570. https://doi.org/10.1159/000373971.

Ye, T., Wang, T., Yang, X., Fan, X., Wen, M., Shen, Y., Xi, X., Men, R., Yang, L., 2018. Comparison of concanavalin a-induced murine autoimmune hepatitis models. Cell. Physiol. Biochem. 46, 1241–1251. https://doi.org/10.1159/000489074.

Yu, J., Ip, E., Dela Peña, A., Hou, J.Y., Sesha, J., Pera, N., Hall, P., Kirsch, R., Leclercq, I., Farrell, G.C., 2006. COX-2 induction in mice with experimental nutritional steatohepatitis: Role as pro-inflammatory mediator. Hepatology 43, 826–836. https://doi.org/10.1002/hep.21108.

Zeng, H., Qian, H.Q., Liang, Z.C., Yang, Y.J., Chu, H.B., Zhang, Y. H., Yao, G.M., 2013. Chemical constituents in twigs and leaves of *Rhododendron fortunei*. Chinese Trad. Herb. Drugs 44, 3123–3126.

Zhang, J.H., Wu, Z., Chen, Z.W., 2007. Protective effect of total flavones of *Rhdodendra* pharmacological preconditioning against inflammation of rat myocardium induced ischemia and reperfusion injury. Chinese Pharmacol. Bull. 23, 1349–1352.

Zhang, P., Yin, Y., Wang, T., Li, W., Li, C., Zeng, X., Yang, W., Zhang, R., Tang, Y., Shi, L., Li, R., Tao, K., 2020. Maresin 1 mitigates concanavalin A-induced acute liver injury in mice by inhibiting ROS-mediated activation of NF-κB signaling. Free Radic. Biol. Med. 147, 23–36. https://doi.org/10.1016/j.freeradbiomed.2019.11.033.

Zhou, Z.H., Yang, C.R., 2000. Chemical constituents of crude green tea, the material of pu-er tea in Yunnan. Acta Bot. Yunnanica 22, 343–350.